SIAM J. APPL. MATH.
Vol. 58, No. 2, pp. 428–455, April 1998

004

CRACK TIP INTERPOLATION, REVISITED*

L. J. GRAY† AND GLAUCIO H. PAULINO‡

Abstract. It is well known that the near tip displacement field on a crack surface can be represented in a power series in the variable $\sqrt{r}$, where r is the distance to the tip. It is shown herein that the coefficients of the linear terms on the two sides of the crack are equal. Equivalently, the linear term in the crack opening displacement vanishes. The proof is a completely general argument, valid for an arbitrary (e.g., multiple, nonplanar) crack configuration and applied boundary conditions. Moreover, the argument holds for other equations, such as Laplace. A limit procedure for calculating the surface stress in the form of a hypersingular boundary integral equation is employed to enforce the boundary conditions along the crack faces. Evaluation of the finite surface stress and examination of potentially singular terms lead to the result. Inclusion of this constraint in numerical calculations should result in a more accurate approximation of the displacement and stress fields in the tip region, and thus a more accurate evaluation of stress intensity factors.

Key words. fracture mechanics, stress intensity factors, crack tip interpolation, hypersingular boundary integrals, eigenfunction expansion

AMS subject classifications. Primary, 73C99; Secondary, 35C10, 35C15, 73V05, 73V10

PII. S0036139996279166

1. Introduction.

In the numerical modeling of fracture, a correct representation of the local stress and displacement fields in the crack tip region is essential for accurate evaluation of stress intensity factors (SIFs). The determination of these quantities is a primary objective of computational fracture mechanics, as they are important for the study of crack stability and propagation [42]. It is therefore not surprising that the analytic form of these singular fields and the associated numerical interpolation methods have received considerable attention.

For two-dimensional linear elasticity, Williams derived the form of the displacement and stress fields in the vicinity of a corner [57] and, subsequently, the limiting case of a crack tip [58]. For recent work on corner expansions, see [9] and references therein. For a crack geometry, Williams's result for the displacement $\mathbf{u} = \{u_k\}$, $k = 1, 2$, in the neighborhood of the tip is

$$u_k(r,\theta) = a_k + b_k(\theta) r^{\frac{1}{2}} + c_k(\theta) r + \mathcal{O}\left(r^{\frac{3}{2}}\right) , \tag{1}$$

where, as illustrated by Fig. 1, r is the distance to the crack tip and θ indicates a direction emanating from the tip. In this figure, the mathematical crack results when the interior angle occupied by the material is 2π (i.e., $\alpha = \pi$) and the crack surfaces correspond to $\theta = \pm\, \pi$. In both finite and boundary element formulations, attention has appropriately focused on capturing the $\sqrt{r}$ behavior (and the corresponding $1/\sqrt{r}$ singularity in the stress field) in the approximation. The development of the "quarter

*Received by the editors February 7, 1996; accepted for publication (in revised form) October 10, 1996. This research was supported by the U. S. Department of Energy, Defense Programs Office of Economic Competitiveness National Information Infrastructure Major Partnership, under contract DE-AC05-84OR21400 with Martin Marietta Energy Systems, Inc.
http://www.siam.org/journals/siap/58-2/27916.html
†Computer Science and Mathematics Division, Oak Ridge National Laboratory, Oak Ridge, TN 37831-6367 (ljg@ornl.gov).
‡Department of Civil and Environmental Engineering, University of California, Davis, CA 95616-5294 (ghpaulino@ucdavis.edu).

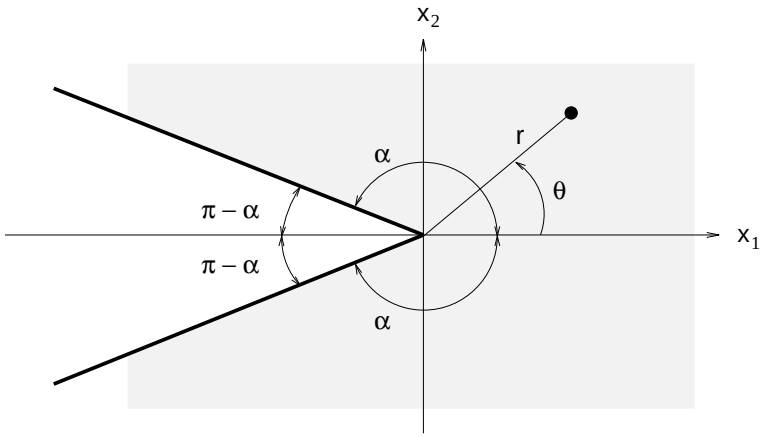

FIG. 1. *Definition of the coordinate systems* $(x_1,\ x_2)$ *and* $(r,\ \theta)$ *for a notch or crack geometry. The shaded portion represents the interior of the domain.*

point" element [5, 30] superseded earlier work in this area (e.g., [55]), and this is now the dominant technique employed. It is well established that use of special elements at the crack tip significantly improves the accuracy of stress intensity factor calculations [3, 8, 37, 49], and many refinements and extensions of the original quarter point element technique have been developed [32, 36] (see also the extensive list of references in [3]). Note that for boundary integral fracture analysis, whether using an approach which combines the displacement and traction boundary integral equations [22, 27, 31] or using the displacement discontinuity method [15, 16, 18, 47], only the displacement *on the crack surfaces*, $\theta = \pm\pi$, is approximated in the calculation. The near tip crack surface interpolation of the displacement is therefore crucial for accurate SIF calculations using these methods.

The purpose of this paper is to establish a relationship between the displacement functions on the top ($\theta = \pi$) and bottom ($\theta = -\pi$) of the crack. Specifically, it will be shown that the coefficients of the linear terms in (1) are related by

$$c_k(\pi) = c_k(-\pi)\ . \tag{2}$$

Note that this equation simply states that there is no linear term present in the expansion of the crack opening displacements, $\Delta\mathbf{u}(r) = \mathbf{u}(r,\pi) - \mathbf{u}(r,-\pi)$. Thus, incorporating (2) into a computational algorithm should be an especially easy task within the displacement discontinuity method [15, 47] or the recent combination of the hypersingular equation method with a symmetric-Galerkin approximation [24]. In both approaches, $\Delta\mathbf{u}(r)$ is dealt with directly.

Given the importance and interest in fracture mechanics, it is somewhat surprising that this simple analytical result, (2), should go unobserved for so long. The proof is based upon the boundary integral formulation for elasticity and the evaluation of the limiting value of the surface stress as the crack tip is approached. A direct computation of the hypersingular integrals, the onerous calculations enormously simplified by employing symbolic manipulation, reveals a logarithmic singularity which vanishes only if (2) holds. Before describing this method, it is useful to demonstrate that the result also follows quite simply from Williams's eigenfunction expansion [57] (section 2). We emphasize, however, that the eigenfunction analysis is restricted to *a traction-free*

flat crack in an infinite plate, whereas the boundary integral derivation (section 3) makes it clear that (2) holds *for an arbitrary crack geometry* and any two-dimensional problem (e.g., potential theory, elastodynamics) for which a boundary integral equation can be constructed. The only assumption in this argument is that the displacement can be represented by (1). The simplifying assumptions in the eigenfunction expansion do yield more detailed information, specifically $c_2(\pi) = c_2(-\pi) = 0$. Crack geometries are of considerable interest in potential theory; thus, section 3 begins with an analysis of the simpler case of crack tip integrals for the Laplace equation. Not surprisingly, the analysis and results for potential and elasticity theory follow along the same lines. In section 4, the validity of (2) is examined for several crack problems having known exact solutions. Section 5 contains some concluding remarks, and a listing of the symbolic integration codes is included in the appendix.

The appearance of the condition in (2) and its derivation from a boundary integral formulation are not unexpected. The interpolation constraint and the method of analysis are natural extensions, to the limiting case of a crack, of previous work dealing with corner geometries [25, 26] (see also [45, 46]). In particular, the *limit to the boundary* process used below to enforce the traction boundary conditions on the crack faces is essentially the same as employed in [25]. In the gradient boundary integral equation for a corner geometry, both integrals (e.g., potential (resp., displacement) multiplying the hypersingular kernel and flux (traction) multiplying the singular kernel in potential (elasticity) theory) contribute logarithmic terms as the interior point approaches the corner. When the corner collapses to a crack, the logarithmic singularity arises only from the hypersingular integral. Moreover, the integrals over the two sides of the crack tip differ by at most a sign, due to the reversal of orientation; thus, unlike the corner problem, there is only one surface integration to contend with.

2. Eigenfunction expansion method. This section presents a proof of the constraint (2) for two-dimensional elasticity based upon the eigenfunction method. This method is especially suitable for representing the elastostatic singularity in a corner region (see Fig. 1) and has strong theoretical support. In particular, Gregory [28] has proven that the Williams's eigenfunctions are complete for the annular sector, an issue of both computational and analytical importance. A general theory of boundary value problems for elliptic equations in domains with angular/conical points has been presented by Kondrat'ev [35]. The present analysis utilizes the real variables theory and follows the general framework presented by Williams [57]. The elegant complex variable formalism of Muskhelishvili [40] is also applicable (e.g., [19, 33, 56]), but this technique does not extend directly to three dimensions, and therefore has not been employed.

For the sake of clarity and completeness, a detailed analysis is presented. The general solution of the eigenproblem, commonly presented in the literature, is *not* valid for the eigenvalues $\lambda = 0$ and $\lambda = \pm 1$ [53, 56], and for the purposes of this paper, it is the case $\lambda = 1$ which is of primary interest. Some authors regard $\lambda = 1$ as a trivial case representing rigid body motion (rotations) [1, p. 27], [34, p. 416]; however, such is not the case for a crack situation ($\alpha = \pi$ in Fig. 1). Thus, the eigenfunctions associated with $\lambda = 1$ are of importance for analyzing the near crack tip fields.

Stress analysis. Let Φ be the *Airy stress function* (e.g., [21, 40]) in polar coordinates (r, θ). In the absence of body forces, the elasticity equations are satisfied if the stresses are derived from Φ according to

$$\begin{aligned}
\sigma_{rr}(r,\theta) &= \frac{1}{r}\frac{\partial\Phi}{\partial r} + \frac{1}{r^2}\frac{\partial^2\Phi}{\partial\theta^2}, \\
\sigma_{\theta\theta}(r,\theta) &= \frac{\partial^2\Phi}{\partial r^2}, \\
\sigma_{r\theta}(r,\theta) &= -\frac{\partial}{\partial r}\left(\frac{1}{r}\frac{\partial\Phi}{\partial\theta}\right) = \frac{1}{r^2}\frac{\partial\Phi}{\partial\theta} - \frac{1}{r}\frac{\partial^2\Phi}{\partial r\partial\theta} \quad ,
\end{aligned} \tag{3}$$

and Φ satisfies the biharmonic equation $\nabla^2(\nabla^2\Phi) = 0$. As usual, ∇^2 denotes the Laplacian

$$\nabla^2 = \frac{\partial^2}{\partial r^2} + \frac{1}{r}\frac{\partial}{\partial r} + \frac{1}{r^2}\frac{\partial^2}{\partial\theta^2}. \tag{4}$$

For the reentrant corner configuration shown in Fig. 1, the Airy stress function can be taken as

$$\Phi = \Phi(r,\theta) = r^{\lambda+1}F(\theta) \ , \tag{5}$$

and substitution of (5) into the biharmonic equation yields (the primes denoting differentiation with respect to θ)

$$F''''(\theta) + 2(\lambda^2+1)F''(\theta) + (\lambda-1)^2(\lambda+1)^2F(\theta) = 0. \tag{6}$$

The general solution of this differential equation is, for $\lambda \neq \{0, 1, -1\}$,

$$F(\theta) = C_1\sin(\lambda+1)\theta + C_2\cos(\lambda+1)\theta + C_3\sin(\lambda-1)\theta + C_4\cos(\lambda-1)\theta. \tag{7}$$

The solutions for the special cases are

$$F(\theta) = C_1\sin\theta + C_2\theta\sin\theta + C_3\cos\theta + C_4\theta\cos\theta \ \text{ for } \ \lambda = 0 \ , \tag{8}$$

$$F(\theta) = C_1 + C_2\theta + C_3\sin 2\theta + C_4\cos 2\theta \ \text{ for } \ \lambda = \pm 1 \ . \tag{9}$$

From (3) and (5) we arrive at the desired form for the stress,

$$\begin{aligned}
\sigma_{rr} &= r^{\lambda-1}\left[F''(\theta) + (\lambda+1)F(\theta)\right], \\
\sigma_{\theta\theta} &= r^{\lambda-1}\left[\lambda(\lambda+1)F(\theta)\right], \\
\sigma_{r\theta} &= r^{\lambda-1}\left[-\lambda F'(\theta)\right].
\end{aligned} \tag{10}$$

In general, the eigenvalues λ and the coefficients C_i $(1 \le i \le 4)$ are complex, and they are determined so that the boundary conditions on the faces of the corner are satisfied. In this section, we are interested in traction-free boundary conditions on the notch faces. Eigenequations for other boundary conditions for corner geometries (clamped-clamped, clamped-free, and free-free) have been investigated by Williams [57].

Eigenvalues. The traction-free boundary conditions on the notch faces (see Fig. 1) are $\sigma_{\theta\theta}(r,\pm\alpha) = 0$ and $\sigma_{r\theta}(r,\pm\alpha) = 0$; thus from (10) it follows that $F(\pm\alpha) = F'(\pm\alpha) = 0$. Applying these conditions to the general solution for F, (7) results in a linear system of four equations in four unknowns, which is easily seen to be equivalent to a pair of uncoupled systems,

$$\begin{bmatrix} \cos(\lambda+1)\alpha & \cos(\lambda-1)\alpha \\ (\lambda+1)\sin(\lambda+1)\alpha & (\lambda-1)\sin(\lambda-1)\alpha \end{bmatrix} \begin{Bmatrix} C_2 \\ C_4 \end{Bmatrix} = \begin{Bmatrix} 0 \\ 0 \end{Bmatrix} \tag{11}$$

and

$$\begin{bmatrix} \sin(\lambda+1)\alpha & \sin(\lambda-1)\alpha \\ (\lambda+1)\cos(\lambda+1)\alpha & (\lambda-1)\cos(\lambda-1)\alpha \end{bmatrix} \begin{Bmatrix} C_1 \\ C_3 \end{Bmatrix} = \begin{Bmatrix} 0 \\ 0 \end{Bmatrix}. \tag{12}$$

A nontrivial solution exists if the corresponding determinants vanish. After simplification, the resulting characteristic equations for the systems (11) and (12) are

$$\lambda \sin 2\alpha + \sin 2\lambda\alpha = 0, \tag{13}$$

$$\lambda \sin 2\alpha - \sin 2\lambda\alpha = 0\ , \tag{14}$$

where the eigenequation (13) is associated with the symmetric part of the solution (opening mode or mode I), the eigenequation (14) is associated with the antisymmetric part (sliding mode or mode II), and the terminology for modes I and II has been borrowed from the fracture mechanics literature. If λ is a solution of either (13) or (14), then $-\lambda$ is also a solution. However, the corresponding stress field has finite strain energy only if $\Re\{\lambda\} > 0$ ($\Re\{\cdot\}$ denotes the real part of the argument); thus only solutions satisfying this inequality need to be considered.

For a crack, $\alpha = \pi$, and (13) or (14) simplify to

$$\sin 2\pi\lambda^I = \sin 2\pi\lambda^{II} = 0, \tag{15}$$

where λ^I and λ^{II} refer to the mode I and mode II eigenvalues, resp. The solution of (15) is

$$\lambda_n^I = \lambda_n^{II} = \lambda_n = \frac{n}{2}, \quad n = 0, 1, 2, 3, \dots\ , \tag{16}$$

where λ_n denotes the nth eigenvalue. As noted above, the cases $\lambda = 0, 1$ (or $n = 0, 2$) are treated separately. In general, the eigenvalues λ_n^I and λ_n^{II} cannot be obtained in a simple form as in (16). A detailed investigation of the behavior of the roots of the characteristic equations (13) and (14) has been presented by Rösel [44] and Vasilopoulos [56].

Displacements. To establish (2), it is necessary to derive the form of the displacements at the crack tip. The polar displacement components (u_r, u_θ) in the radial and circumferential directions (see Fig. 1) can be expressed as

$$\begin{aligned} u_r &= \frac{1}{2\mu}\left[-\frac{\partial\Phi}{\partial r} + (1-\varsigma) r \frac{\partial\Psi}{\partial\theta}\right], \\ u_\theta &= \frac{1}{2\mu}\left[-\frac{1}{r}\frac{\partial\Phi}{\partial\theta} + (1-\varsigma) r^2 \frac{\partial\Psi}{\partial r}\right], \end{aligned} \tag{17}$$

resp., where μ is the shear modulus, $\varsigma \equiv \nu$ for plane strain, $\varsigma \equiv \nu/(1+\nu)$ for plane stress, and ν is the Poisson's ratio. The function Ψ satisfies the Laplace equation $\nabla^2\Psi = 0$ and, in addition, is related to the biharmonic function Φ by [14, pages 166–168]

$$\nabla^2\Phi = \frac{\partial}{\partial r}\left(r\frac{\partial\Psi}{\partial\theta}\right). \tag{18}$$

Applying the eigenanalysis to Ψ,

$$\Psi = \Psi(r,\theta) = r^m G(\theta). \tag{19}$$

Substituting this into the Laplace equation it is seen that $G(\theta)$ satisfies the differential equation

$$m^2 G(\theta) + G''(\theta) = 0 \tag{20}$$

and is therefore of the form

$$G(\theta) = A_1 \cos m\theta + A_2 \sin m\theta, \tag{21}$$

where m is, in general, complex. Moreover, (18) provides a connection between the expressions for G and F (7), and equating the powers of r and like trigonometric terms yields

$$\lambda = m + 1\,, \quad A_1 = -\frac{4}{\lambda - 1} C_3, \quad \text{and} \quad A_2 = \frac{4}{\lambda - 1} C_4. \tag{22}$$

Substitution of these results into (21) leads to

$$G(\theta) = \frac{4}{\lambda - 1}\left[-C_3 \cos(\lambda - 1)\theta + C_4 \sin(\lambda - 1)\theta\right]. \tag{23}$$

Finally, combining (5), (19), and (17) yields the displacement components

$$\begin{aligned} 2\mu u_r &= r^\lambda \left[-(\lambda + 1)F(\theta) + (1 - \varsigma)G'(\theta)\right], \\ 2\mu u_\theta &= r^\lambda \left[-F'(\theta) + (1 - \varsigma)(\lambda - 1)G(\theta)\right]. \end{aligned} \tag{24}$$

Remarks. The eigenequations (13) and (14) have been derived from (7), which is not valid for $\lambda = 0,\ \pm\ 1$. As noted previously, these eigenvalues must be treated separately. The case $\lambda = -1$ is not physically meaningful,while it follows from (9) that $\lambda = 0$ represents the trivial case for which all the stresses are zero and the displacements are rigid body translations.

It is interesting to note that the coefficients of the square root term, $u_k = b_k\sqrt{r},\ k = 1, 2$, on the top and bottom of the crack surfaces are related by

$$b_k(\pi) = -b_k(-\pi). \tag{25}$$

This follows from the general form of the displacement with $\lambda = \lambda_1 = 1/2$, (24), and is a consequence of the symmetry of the domain and boundary conditions. The case $\lambda = 1$ is directly related to the proposed constraint (2) and will now be investigated in detail.

Linear mode. When $\lambda = 1$, the Airy stress function, (5), becomes

$$\Phi = r^2 F(\theta), \tag{26}$$

where $F(\theta)$ is given by (9). Also, $m = 0$, and thus the form of the harmonic function $G(\theta)$ is simply

$$\Psi = G(\theta) = A_1 + A_2\theta, \tag{27}$$

and from (18),

$$A_2 = 4C_1 \qquad \text{and} \qquad C_2 = 0. \tag{28}$$

Substitution of (26), (9), and (28) in (3) leads to the stress field

$$\begin{aligned} \sigma_{rr} &= 2C_1, \\ \sigma_{\theta\theta} &= 2\left(C_1 + C_3 \sin 2\theta + C_4 \cos 2\theta\right), \\ \sigma_{r\theta} &= -2\left(C_3 \cos 2\theta - C_4 \sin 2\theta\right), \end{aligned} \tag{29}$$

from which the traction-free boundary conditions give

$$\begin{aligned} C_1 + C_4 \cos 2\alpha = 0, \qquad & C_3 \sin 2\alpha = 0, \\ C_3 \cos 2\alpha = 0, \qquad & C_4 \sin 2\alpha = 0. \end{aligned} \tag{30}$$

Thus, $C_3 = 0$, and specializing these results for a crack ($\alpha = \pi$), $C_1 = -C_4$. Substituting these results for the C_i's and (26) and (27) into (17), one obtains the polar displacement components

$$\begin{aligned} u_r &= -r\frac{1}{2\mu} C_4 \left(\kappa - 1 + 2\cos 2\theta\right), \\ u_\theta &= r\frac{1}{\mu} C_4 \sin 2\theta, \end{aligned} \tag{31}$$

where $\kappa \equiv 3 - 4\varsigma$. By (31) these represent mode I displacements. In Cartesian coordinates, these displacement components are

$$\begin{aligned} u_1 &= -r\frac{1}{2\mu} C_4 \left(\kappa + 1\right) \cos\theta, \\ u_2 &= -r\frac{1}{2\mu} C_4 \left(\kappa - 3\right) \sin\theta \ . \end{aligned} \tag{32}$$

These equations are of the form $u_k = c_k r$, $k = 1, 2$, and it is readily seen that the coefficients on the top ($\theta = \pi$) and bottom ($\theta = -\pi$) of the crack surfaces are

$$\begin{aligned} c_1(\pi) = c_1(-\pi) &= \frac{1}{2\mu} C_4(\kappa + 1), \\ c_2(\pi) = c_2(-\pi) &= 0 \ . \end{aligned} \tag{33}$$

Therefore, the proposed constraint on the crack faces, (2), is in agreement with the results by the eigenfunction expansion, (33).

3. Boundary integral analysis. The proof of (2) which follows relies on direct evaluation of the crack tip integral in the hypersingular boundary integral equation for the surface derivatives. Note that the symmetry arguments, which underlie Williams's asymptotic expansion of the stress [20, (2)], are *not* required for this analysis. The singular integrals are defined in terms of a limit process which is consistent with the physics of the problem, namely that the limit to the crack tip be taken *along the crack surface* (see Fig. 2). Whereas the boundary conditions demand that this value remains finite as the boundary point approaches the tip, the calculation produces a logarithmic singularity. This singularity only vanishes if (2) holds.

The limit analysis presented herein is similar to the work by Cruse [17] in establishing the form of the stress field ahead of the crack. His calculations evaluated the

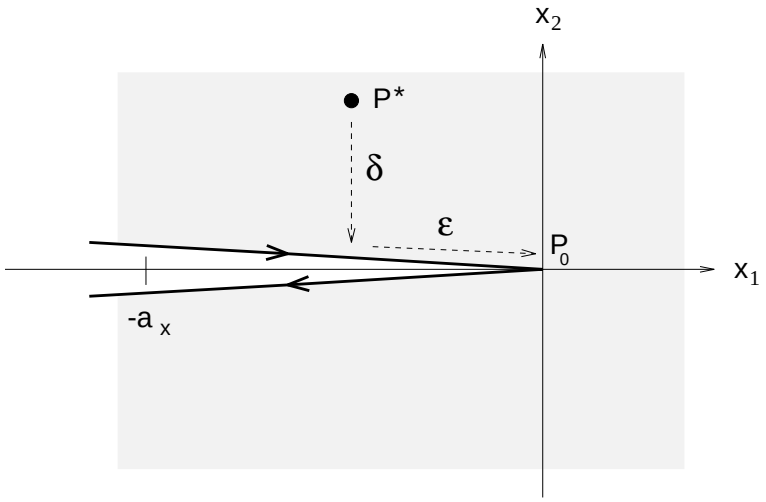

FIG. 2. *Illustration of the double limit process.*

stress in *the interior of the domain*, at a point ahead of and approaching the tip. As indicated above, the limit process employed below also involves evaluating the stress near the tip, but now on the crack surface.

As indicated in the introduction, this argument is not restricted to elasticity. The simplest formulation (and integrations) are for the two-dimensional Laplace equation $\nabla^2\phi = 0$, for which the potential ϕ and its normal derivative play the role of the displacement and traction in elasticity. The boundary integral proof will therefore be presented first in this simpler setting, and then for the linear theory of elasticity (i.e., linear elastic fracture mechanics).

In what follows, it is *assumed* that the potential or displacement *on the crack surface* follows Williams's result, (1), for an isolated traction-free crack in an infinite medium. Specifically, the near tip behavior will be represented by the expansion

$$u_k(r, \pm\,\pi) = a_k + b_k(\pm\,\pi)r^{\frac{1}{2}} + c_k(\pm\,\pi)r + \mathcal{O}\left(r^{\frac{3}{2}}\right) \ . \tag{34}$$

For our purposes, it is important that $\lambda = 1/2$ be the only exponent in this series in the interval $0 < \lambda < 1$. This is in fact the basis for employing stress intensity factors as characterizing parameters for fracture analysis.

3.1. Potential theory. Aside from simplicity, there is another important reason for examining the Laplace equation. While probably not studied as extensively as linear elastic fracture mechanics, crack problems in potential theory are nevertheless of considerable interest [2]. Specific applications are in electroplating [12, 22], wherein the crack is generally thin, insulated shielding, and in groundwater flow models containing either fractures [39, 48] or thin impermeable layers [52]. Moreover, the antiplane shear crack problem in a linearly elastic solid is also governed by the (two-dimensional) Laplacian operator (see, for example, [41]).

The boundary integral equation for two-dimensional potential theory can be written as [25]

$$\phi(P) + \int_{\partial B} \phi(Q)\frac{\partial G}{\partial \mathbf{n}}(P,Q)\,dQ = \int_{\partial B} G(P,Q)\frac{\partial \phi}{\partial \mathbf{n}}\,dQ \ , \tag{35}$$

where ϕ is the potential, $\mathbf{n}$ is the unit outward normal on the boundary ∂B, and $\partial(\cdot)/\partial\mathbf{n}$ denotes the normal derivative with respect to Q. The fundamental solution or Green's function will be taken as the point source potential

$$G(P,Q) = -\frac{1}{2\pi}\log\|Q-P\| \ . \tag{36}$$

Note that (35) holds for a point $P \in B$ interior to the domain, *and, defining the singular integrals* (which arise when $P = Q$) *in terms of a limit to the boundary* [22], *also for* $P \in \partial B$ [38].

Differentiating (35) with respect to P in the direction $\mathbf{N} = \mathbf{n}(P)$ results in a corresponding equation for surface flux,

$$\frac{\partial\phi}{\partial\mathbf{N}}(P) + \int_{\partial B}\phi(Q)\frac{\partial^2 G}{\partial\mathbf{N}\partial\mathbf{n}}(P,Q)\,dQ = \int_{\partial B}\frac{\partial G}{\partial\mathbf{N}}(P,Q)\frac{\partial\phi}{\partial\mathbf{n}}(Q)\,dQ \ . \tag{37}$$

Once again, this equation is valid for $P \in \partial B$ by defining the singular integrals as a limit from the interior of the domain [22]. The explicit form of the kernel functions is

$$\begin{aligned}\frac{\partial G}{\partial\mathbf{N}}(P,Q) &= \frac{1}{2\pi}\frac{\mathbf{N}\bullet\mathbf{R}}{r^2},\\ \frac{\partial^2 G}{\partial\mathbf{N}\partial\mathbf{n}}(P,Q) &= \frac{1}{2\pi}\left(\frac{\mathbf{n}\bullet\mathbf{N}}{r^2} - 2\frac{(\mathbf{n}\bullet\mathbf{R})(\mathbf{N}\bullet\mathbf{R})}{r^4}\right) \ ,\end{aligned} \tag{38}$$

where $r = \|\mathbf{R}\| = \|Q-P\|$.

The equation for surface flux, (37), will be employed to enforce the flux boundary conditions along the crack faces. As illustrated in Fig. 2, this calculation is carried out by means of a double limiting procedure. The crack lies along the negative x_1-axis, and the flux is calculated at an interior point P^*,

$$P^* = \varepsilon(-1,0) + \delta(0,1) \ . \tag{39}$$

The limits $\delta \to 0$ and $\varepsilon \to 0$ are then considered, *in this order*. Thus, P^* first approaches the crack surface ($y = 0^+$) a small distance ε from the tip, and then the limit $\varepsilon \to 0$ is considered. Since the flux is finite on the crack surface (the usual boundary condition is zero flux), this limit procedure must produce a finite value. In the derivation, only potentially singular terms will be of interest. As shown below, the limiting value flux integral on the right-hand side in (37) is well behaved, and thus this integral can be ignored. Similarly, the hypersingular integral only contributes potentially singular terms for the integration over the crack tip region, the remainder of the boundary producing a finite value as $P^* \to P_0$. Moreover, from (34), it also suffices to consider the first three terms in an expansion for ϕ on the crack surface,

$$\phi = a + b\sqrt{r} + cr \ . \tag{40}$$

For a flat crack, the evaluation of the corresponding three integrals over the crack tip can be carried out analytically. This is most easily accomplished using a symbolic manipulation program such as Maple [13]. The Maple scripts for the integrations discussed below are listed in the appendix.

Although the use of these analytical integrations appears to limit the argument to a flat crack, it should be emphasized that (2) nevertheless remains valid for any smooth curved crack. A simple heuristic justification of this statement is that the proof relies

solely on integrals over an arbitrarily small crack tip region, and any smooth surface is locally flat. A rigorous argument can be based upon the techniques presented in [23], which demonstrate that the difference between integrating (hyper)singular boundary integrals over flat and curved surfaces is a completely regular integral (see also [24]). Once again, only potentially singular contributions are of interest, and thus there is no loss of generality in restricting consideration to a flat crack.

It is assumed that, as shown in Fig. 2, the domain of integration (crack tip element) is $[-a_x, 0]$, $a_x > 0$, parameterized as $Q(x) = (a_x x, 0)$, $-1 \le x \le 0$. The crack tip is $P_0 = (0,0)$. The interior point P in (37) is taken as $P^* = (-\varepsilon, \delta)$. After the integral is evaluated, the limit to the crack surface, $\delta \to 0$, is computed, and then the approach to the crack tip, $\varepsilon \to 0$, is considered. As noted above, this procedure is easily carried out using symbolic computation. Note that the integrations over the top $y = 0^+$ and bottom $y = 0^-$ of the crack only differ by a sign, and thus it is sufficient to integrate over the top surface. From (38), and with $\mathbf{n} = \mathbf{N} = (0,1)$ on the top crack surface $y = 0^+$, the integrals to be computed in (37) are

$$\lim_{\varepsilon\to 0}\lim_{\delta\to 0}\left(-\frac{1}{2\pi}\right)\int_{-1}^{0}\left(a+b\sqrt{x}+cx\right)\frac{2a_x\delta^2-a_x\left(\left(a_x x+\varepsilon\right)^2+\delta^2\right)}{\left(\left(a_x x+\varepsilon\right)^2+\delta^2\right)^2}\,dx\ ,$$

$$\lim_{\varepsilon\to 0}\lim_{\delta\to 0}\left(-\frac{1}{2\pi}\right)\int_{-1}^{0}\frac{-a_x\delta}{\left(a_x x+\varepsilon\right)^2+\delta^2}\,dx\ . \tag{41}$$

Note that in the expansion for $\partial\phi/\partial\mathbf{n}$ in the second integral above, only the constant term has been considered, as this is the only term that can contribute potentially singular terms in the limit process. The three terms involving the coefficients $\{a, b, c\}$ in the first integral, and the second integral in (41), are considered separately below.

Constant: $\boldsymbol{\phi = a}$. The integral over one side of the crack surface evaluates as

$$-\frac{a}{2\pi}\left(\frac{1}{\varepsilon}+\frac{1}{a_x}\right)\ . \tag{42}$$

The coefficient a is the same on both sides, and thus the singular ε^{-1} term cancels (as does the finite contribution) with the integration over the second side. Note that this term is not present in a displacement discontinuity approach [15], and thus the canceling of this contribution is entirely reasonable.

Square root: $\boldsymbol{\phi = b\sqrt{x}}$. The integration of the square root term in (41) is more involved and results in significantly longer and more complicated expressions. Moreover, it is not immediately possible, as with the constant and linear terms, to set $\delta = 0$. As indicated by the Maple coding in the Appendix, this limit process is partly simplified by means of the Taylor expansion at $\delta = 0$ (note that δ goes to zero before ε),

$$\sqrt{\varepsilon^2+\delta^2} = \varepsilon + \frac{\delta^2}{2\varepsilon} + \mathcal{O}\left(\delta^4\right)\ . \tag{43}$$

Applying this expansion to the integration of the square root term results in

$$-\frac{b}{2\pi}\left[\frac{1}{a_x}+\frac{1}{4\sqrt{a_x\varepsilon}}\log\left(a_x+2\sqrt{a_x\varepsilon}+\varepsilon\right)\right.$$
$$\left.-\frac{1}{4\sqrt{a_x\varepsilon}}\log\left(a_x-2\sqrt{a_x\varepsilon}+\varepsilon\right)\right]\ . \tag{44}$$

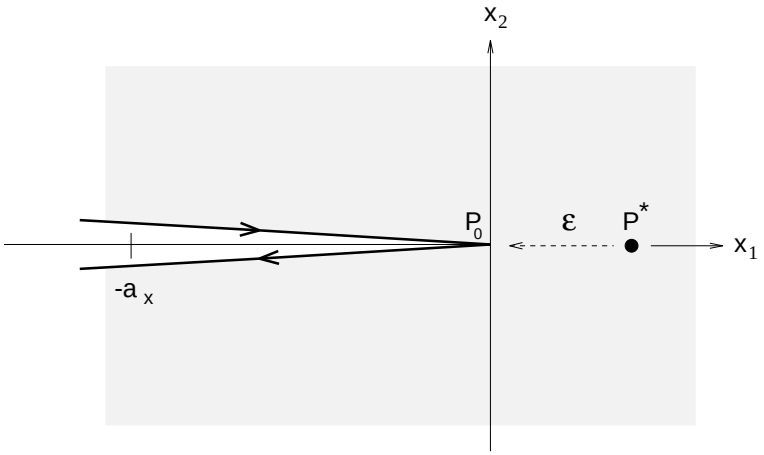

FIG. 3. *Limit process for determining the amplitude of the singular field.*

The logarithmic terms, apparently singular in the $\varepsilon = 0$ limit, can be rewritten, however, as

$$-\frac{b}{8\pi\sqrt{a_x\varepsilon}}\log\left(\frac{1+q}{1-q}\right), \qquad q=\frac{2\sqrt{a_x\varepsilon}}{a_x+\varepsilon}\ , \tag{45}$$

and employing the Taylor expansion at $q = 0$,

$$\log\left(\frac{1+q}{1-q}\right) = 2q + \mathcal{O}\left(q^3\right)\ , \tag{46}$$

now shows that this term is well behaved. Thus, no singular terms arise from the $\sqrt{x}$ term, and the result of the limit procedure is

$$-\frac{b}{\pi a_x}\ . \tag{47}$$

As a final comment, it is worth noting that the flux as P^* approaches the tip from the interior of the domain (i.e., not along the crack surface (Fig. 3)) is, as expected, singular. Taking $P^* = (\varepsilon, 0)$ and evaluating the hypersingular integral, one obtains

$$-\frac{b^+-b^-}{2\pi}\left[\frac{1}{a_x+\varepsilon}-\frac{\tan^{-1}\left(\sqrt{a_x/\varepsilon}\right)}{\sqrt{a_x\varepsilon}}\right] \to -\frac{b^+-b^-}{2\pi}\left[\frac{1}{a_x}-\frac{\pi}{2\sqrt{a_x\varepsilon}}\right]\ , \tag{48}$$

which gives the expected $1/\sqrt{\varepsilon}$ singularity. This particular limit process (Fig. 3) offers the possibility of deriving an effective general method for computing stress intensity factors in the context of linear elastic fracture mechanics. This technique is currently under investigation.

Linear: $\boldsymbol{\phi = cx}$. The announced result, (2), follows from an examination of the integrals for this linear term. Direct evaluation yields

$$-\frac{c}{2\pi}\left(-\frac{\log(\varepsilon^2)}{2a_x}+\frac{\log(a_x^2)-2}{2a_x}\right)\ . \tag{49}$$

Thus, the integration over both sides of the crack produces a singular term of the form

$$-\left(c^+ - c^-\right) \frac{\log(\,|\,\varepsilon\,|\,)}{2\pi a_x}\ , \tag{50}$$

where c^+ and c^- denote the linear coefficients on the two sides. As there are no other singular terms which come out of evaluating the flux at the crack tip, the only way to cancel the singularity in (50) is to have $c^+ = c^-$.

Flux integral. The most common boundary condition on a crack surface is zero flux (zero traction in the case of elasticity). The "flux integral" in the hypersingular equation (37) will therefore not contribute to the evaluation of the flux at the tip. However, in some applications (e.g., pressurized crack) this boundary condition will not be zero, and it is therefore necessary to check whether any singular terms arise from this integration. This is not the case, as is easily seen from examining the lowest order term, $\partial\phi/\partial\mathbf{n} = \alpha_0$, where α_0 is a constant. Evaluating this integral yields

$$-\frac{\alpha_0}{2\pi}\frac{\delta}{|\delta|}\left\{\tan^{-1}\left(\frac{\varepsilon}{\delta}\right) + \tan^{-1}\left(\frac{a_x-\varepsilon}{\delta}\right)\right\}\ . \tag{51}$$

In the limit $\delta \to 0$, the $\tan^{-1}$ terms become $\pi/2$, and thus, as expected, this expression reduces to the usual "interior angle" coefficient $1/2$ for a smooth surface.

3.2. Elasticity theory. The boundary integral proof for elasticity mostly follows along the above lines, and thus only a brief description of the formulation and the results will be given. As will be discussed below, the main difference involves the square root term. The Maple codes for the elasticity integrations are also listed in the Appendix.

The boundary integral equation for two-dimensional elasticity is given by [16, 43]

$$u_k(P) + \int_{\partial B} T_{kj}(P,Q)u_j(Q)\,dQ = \int_{\partial B} U_{kj}(P,Q)\tau_j(Q)\,dQ\ , \tag{52}$$

where $\mathbf{u}$ and $\boldsymbol{\tau}$ denote displacement and traction, respectively. As customary, the kernel functions $T_{kj}(P,Q)$ and $U_{kj}(P,Q)$ are given by the Kelvin solution for a point load in an infinite medium. Eq. (52) holds for a point $P \in B$ interior to the domain, and, defining the singular integrals in terms of a *limit to the boundary* [38], also for $P \in \partial B$. A corresponding equation for the stress can be obtained by differentiating (52) with respect to P [27], resulting in

$$\sigma_{lk}(P) + \int_{\partial B} S_{lkm}(P,Q)u_m(Q)\,dQ = \int_{\partial B} D_{lkm}(P,Q)\tau_m(Q)\,dQ\ . \tag{53}$$

Once again, this equation is valid for $P \in \partial B$ by defining the singular integrals as a limit from the interior of the domain. The new kernels $D_{lkm}(P,Q)$ (singular) and $S_{lkm}(P,Q)$ (hypersingular) are given by [10, (5.69) and (5.70)]

$$\begin{aligned}
D_{lkm} &= \frac{1}{4\pi(1-\nu)r}\left[(1-2\nu)\left\{\delta_{lm}r_{,k} + \delta_{km}r_{,l} - \delta_{lk}r_{,m}\right\} + 2r_{,l}r_{,k}r_{,m}\right],\\
S_{lkm} &= \frac{\mu}{2\pi(1-\nu)r^2}\left[2\frac{\partial r}{\partial \mathbf{n}}\left(\{1-2\nu\}\,\delta_{lk}r_{,m} + \nu\left(\delta_{km}r_{,l} + \delta_{lm}r_{,k}\right) - 4r_{,l}r_{,k}r_{,m}\right)\right.\\
&\qquad + (1-2\nu)\left(2n_m r_{,l}r_{,k} + n_k\delta_{lm} + n_l\delta_{km}\right)\\
&\qquad \left. + 2\nu\left(n_l r_{,k}r_{,m} + n_k r_{,l}r_{,m}\right) - (1-4\nu)n_m\delta_{lk}\right]\ ,
\end{aligned} \tag{54}$$

where ν is Poisson's ratio, μ is shear modulus, δ_{ij} is the Kronecker delta, $r_{,i} = \partial r/\partial q_i$, and q_i is the ith coordinate of the field point Q. As in potential theory, there is no contribution, singular or otherwise, from the constant term $\mathbf{u} = \mathbf{u}(P_0)$ in the hypersingular displacement integral. This value is the same on both sides of the crack, and the singular integrals are continuous crossing the boundary. Thus, the opposite orientation of the two crack tip elements ensures that the two integrals cancel, and it suffices to examine the square root and linear coefficient terms. For the traction integral, once again only the constant term is of interest. The integrals to be computed are therefore

$$\lim_{\varepsilon\to 0}\lim_{\delta\to 0}\int_{-1}^{0}\left(b_m\sqrt{x}+c_m x\right)S_{lkm}\left(P^*,Q(x)\right)\,dx,$$

$$\lim_{\varepsilon\to 0}\lim_{\delta\to 0}\int_{-1}^{0}D_{lkm}\left(P^*,Q(x)\right)\,dx\ . \tag{55}$$

Square root: $u_k = b_k\sqrt{r}$. The analysis of this term differs from that in potential theory in that the Taylor expansion, (43), must include an additional term,

$$\sqrt{\varepsilon^2+\delta^2} = \varepsilon\left(1+\frac{\delta^2}{2\varepsilon^2}-\frac{\delta^4}{8\varepsilon^4}\right)+\mathcal{O}\left(\delta^6\right)\ . \tag{56}$$

Fortunately, all of the lengthy algebra which results is easily handled via symbolic computation. For $\mathbf{N} = (0,1)$, the traction vector on the crack surface is $\boldsymbol{\tau} = (\sigma_{12},\sigma_{22})$ and the calculation yields the simple result

$$\boldsymbol{\tau} = -\frac{\mu}{2\pi(1-\nu)a_x}\left\{\begin{array}{c} b_1 \\ b_2 \end{array}\right\}\ . \tag{57}$$

Thus, as in potential theory, elasticity does not impose any relationship between the coefficients b^+ and b^-.

Linear: $u_k = c_k r$. The potentially singular terms which arise in the evaluation of the crack tip limits are

$$\begin{aligned}\tau_1 = \sigma_{12} &= \frac{\mu}{\pi(1-\nu)a_x}\left(c_1^+ - c_1^-\right)\log(\,\varepsilon\,),\\ \tau_2 = \sigma_{22} &= \frac{\mu}{\pi(1-\nu)a_x}\left(c_2^+ - c_2^-\right)\log(\,\varepsilon\,)\ ,\end{aligned} \tag{58}$$

and a finite value at the tip therefore requires that (2) be satisfied.

Traction integral. Pressurized crack problems are of interest in various applications, such as pressure-induced fractures in oil and gas reservoirs [51], and thus the effect of a non-zero boundary condition on the crack will now be investigated (see Fig. 4). England [19] has verified that the crack tip stress singularity for a pressurized crack (finite straight crack in an infinite medium) remains $r^{-1/2}$. Thus, in this case, the form of the displacement remains as in (1).

Evaluation of the constant term in the traction integral yields

$$\begin{aligned}\sigma_{12} &= \frac{1}{4\pi(1-\nu)}\left[\frac{1}{2}\frac{\log(\varepsilon)}{a_x}-\frac{\nu\log(\varepsilon)}{a_x}-\frac{1}{2}\frac{\log(a_x^2)}{a_x}+\frac{\nu\log(a_x^2)}{a_x}\right]\alpha_2,\\ \sigma_{22} &= \frac{1}{4\pi(1-\nu)}\left[-\frac{1}{2}\frac{\log(\varepsilon)}{a_x}+\frac{\nu\log(\varepsilon)}{a_x}+\frac{1}{2}\frac{\log(a_x^2)}{a_x}-\frac{\nu\log(a_x^2)}{a_x}\right]\alpha_1\ ,\end{aligned} \tag{59}$$

where $\alpha_1^+ = \alpha_1^- = \alpha_1$ and $\alpha_2^+ = \alpha_2^- = \alpha_2$ are constants. Cancelation of the potentially singular terms results from adding the contributions from the two sides of the crack.

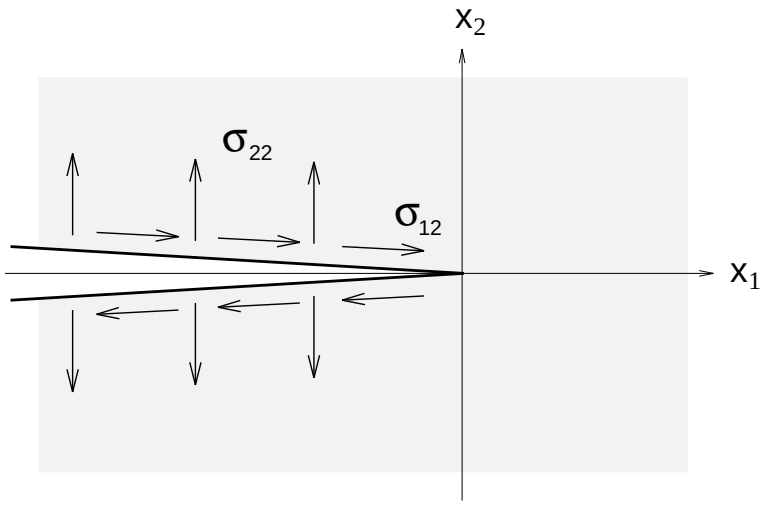

FIG. 4. *Loaded crack.*

4. Exact solutions. In this section we examine several known exact solutions from the well-known compilation of crack problems by Tada, Paris, and Irwin [54] and verify that they satisfy (2). The motivation for doing this verification is that the general boundary integral proof presented above depends upon the assumption that (1) is valid. It will be demonstrated that (2) does in fact hold for a variety of crack geometries and boundary conditions. Moreover, the form of the crack opening $\Delta\mathbf{u}$ varies significantly, and thus these examples lend credence to the belief that (1) and (2) are indeed valid. Nevertheless, keep in mind that since exact solutions exist, all of the problems are necessarily relatively "simple" (e.g., flat cracks and generally possessing some type of symmetry). In particular, see the comment below concerning the coefficient of the r^2 term.

Four example problems will be considered, and they will be identified by the numbering scheme employed in reference [54]. Only the first example is discussed in detail, as the analysis for the remaining three examples follows along the same lines. Again, the required computations, in this case evaluating the second derivative of some complicated functions, are easily accomplished by means of symbolic manipulation. The Maple scripts are included in the appendix, section 6.3.

4.1. Eccentric load on the crack faces. Figure 5 shows an infinite plate containing a straight crack ($-a_x \le x_1 \le a_x$) with eccentric point loads (P) on its faces at $(b, 0^+)$ and $(b, 0^-)$. Note that this example demonstrates that (2) holds even for a point load arbitrarily close to the tip. The crack opening displacement is given by

$$\Delta u_2(x_1, 0) = \frac{4P}{\pi E^*} \cosh^{-1}\left(\frac{a_x^2 - b\,x_1}{a_x|x_1 - b|}\right), \tag{60}$$

where $E^* \equiv E/(1-\nu)^2$ for plane strain and $E^* \equiv E$ for plane stress.

To compute the coefficient of the linear term in the expansion at the crack tip $x_1 = a_x$ we first make the substitution $r = a_x - x_1$, r being the distance to the crack tip, and since the leading term is $\sqrt{r}$, we further substitute $s^2 = r$. The desired coefficient of the linear term in r is therefore the coefficient of s^2 in the Taylor

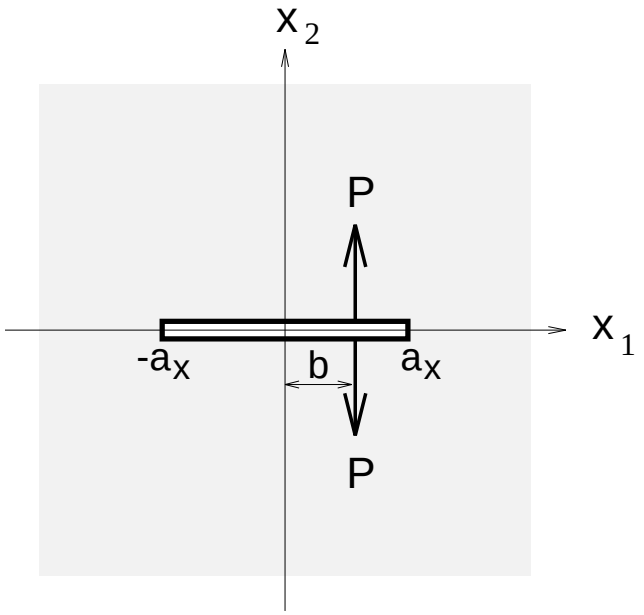

FIG. 5. *Example* 5.10*a from Tada, Paris, and Irwin* [54].

expansion about $s = 0$ for the function

$$f(s) = \frac{4P}{\pi E^*} \cosh^{-1}\left(\frac{1+\beta\, s^2}{1-\alpha\, s^2}\right), \tag{61}$$

where $\alpha = 1/(a_x - b)$ and $\beta = b\,\alpha/a_x$, and this coefficient is easily computed as $f''(0)/2$. As indicated by the Maple code in the appendix, $f''(s)$ is written in the form $A(s)/B(s)$, and employing Taylor expansions for both numerator and denominator yields

$$f''(s) \approx -\frac{16P}{\pi E^*} \frac{(\,\beta^2 - 4\,\beta\,\alpha - 5\,\alpha^2\,)\,s}{(\,3\,\beta\, s^2 + 4 - 11\,\alpha\, s^2\,)\sqrt{2\,\beta + 2\,\alpha}}, \tag{62}$$

and as desired, $f''(0) = 0$. Moreover, evaluation of the leading terms shows that

$$\begin{aligned}\Delta u_2(r) = \frac{4P}{\pi E^*}\Bigg(&\frac{\sqrt{2}}{\sqrt{a_x}}\frac{\sqrt{a_x^2 - b^2}}{a_x - b}\, r^{1/2} \\ &2\,\frac{5\alpha^4 + 14\beta\alpha^3 + 12\beta^2\alpha^2 + 2\beta^3\alpha - \beta^4}{3(2\beta + 2\alpha)^{5/2}}\, r^{3/2} + \mathcal{O}\left(r^{\frac{5}{2}}\right)\Bigg)\ ,\end{aligned} \tag{63}$$

and as the mode I stress intensity factor K_I is $\sqrt{\pi}E^*/4\sqrt{2}$ times the coefficient of $r^{1/2}$ (see Appendix B in [54]), $K_I\,(a_x) = (P/\sqrt{\pi a_x})\,\sqrt{a_x^2 - b^2}\,/\,(a_x - b)$. This agrees with the result reported in [54]. Note too that, as is the case for all four examples, the coefficient of r^2 is also zero.

The analysis for the crack tip at $x_1 = -a_x$ proceeds in much the same fashion, only now $r = a_x + x_1$, and

$$f(s) = \frac{4P}{\pi E^*} \cosh^{-1}\left(\frac{1-\beta^*\, s^2}{1-\alpha^*\, s^2}\right), \tag{64}$$

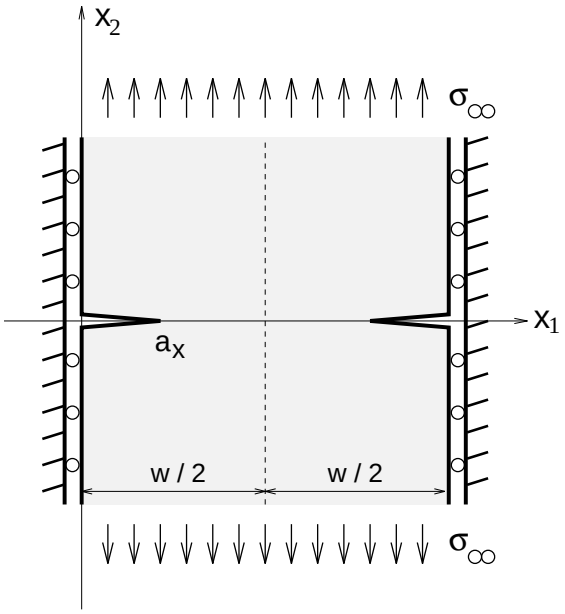

FIG. 6. *Example* 7.1*a from Tada, Paris, and Irwin* [54].

$\alpha^* = 1/(a_x + b)$, and $\beta^* = b\,\alpha^*/a_x$. Finally, note that an arbitrary traction boundary condition on the crack surface can be represented as a continuous distribution of point sources, and thus the r coefficient should be zero in this case as well. This can be directly observed from the exact solution obtained by Sneddon and Elliott [50].

4.2. Strip with edge cracks remotely loaded. Figure 6 shows an infinite strip (width $= W$) with edge cracks subjected to remote tension loading (σ_∞). Note that, due to the boundary conditions, the crack opening displacement for the crack on the left ($\Delta u_2(x_1, 0),\ 0 \le x_1 \le a_x$) is the same as the crack opening displacement for the right-half part of a central crack of length $2a_x$ in an infinite strip subjected to the same remote loading [54]. As the parameters a_x and W are arbitrary, this problem provides a surface crack example where the crack tip is close to the outer boundary and/or close to another crack. The crack opening displacement is

$$\Delta u_2(x_1, 0) = \frac{4\sigma_\infty W}{\pi E^*} \cosh^{-1}\left(\frac{\cos(\pi\, x_1/W)}{\cos(\pi\, a_x/W)}\right), \tag{65}$$

and the symbolic code in the appendix shows that the coefficient of the linear term of the Taylor expansion of this function at $x_1 = a_x$ is zero.

4.3. Strip with central crack and concentric loads. Figure 7 shows an infinite strip (width $= W$) containing a straight crack ($-a_x \le x_1 \le a_x$) with concentric point loads (P) located at $x_2 = \pm y_0$. Again, of primary interest is that the parameters $\{a_x, W, y_0\}$ are arbitrary, and thus for $a_x \approx W/2$, the crack tips strongly interact with the outer boundary. The crack opening displacement is

$$\begin{aligned}\Delta u_2(x_1, 0) = {} & \frac{4P}{\pi E^*}\left(1 - \alpha y_0 \frac{\partial}{\partial y_0}\right) \\ & \times \tanh^{-1}\left(\left[\frac{1 - \left(\cos(a_x\,\pi/W)/\cos(\pi\, x_1/W)\right)^2}{1 - \left(\cos(a_x\,\pi/W)/\cosh(\pi\, y_0/W)\right)^2}\right]^{\frac{1}{2}}\right),\end{aligned} \tag{66}$$

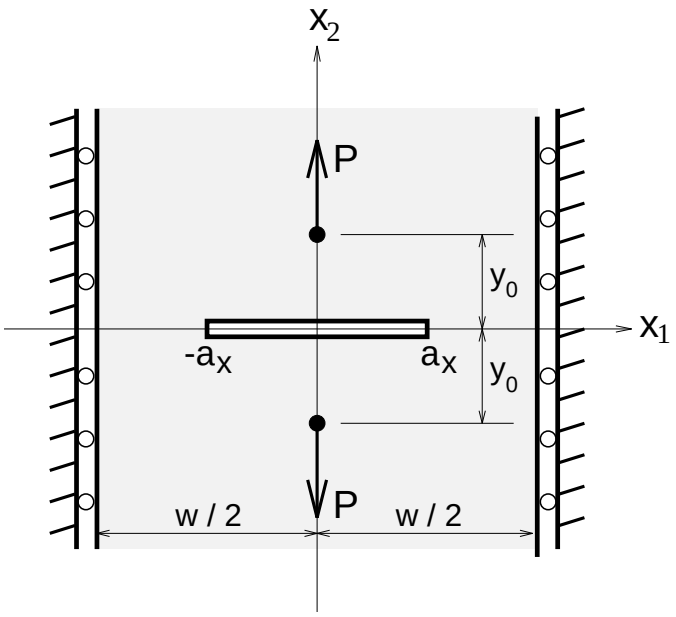

FIG. 7. *Example* 7.4*a from Tada, Paris, and Irwin* [54].

and, again, the symbolic code in the appendix shows that the coefficient of the linear term of the Taylor expansion of this function at $x_1 = a_x$ is zero. By symmetry, the results for the expansions at $x_1 = a_x$ and $x_1 = -a_x$ are the same.

4.4. Parallel cracks remotely loaded in antiplane shear. Figure 8 shows an infinite plate containing parallel straight cracks ($-a_x \leq x_1 \leq a_x$) separated by the distance H and subjected to remote antiplane shear loading (σ_{32}). In addition to providing an example involving multiple interacting cracks, this problem involves the tearing rather than the opening mode. The crack tearing displacement is

$$\Delta u_3(x,0) = \frac{\sigma_{32} H}{G\pi} \cos^{-1}\left(\frac{\cosh(\,\pi\, x_1/H\,)}{\cosh(\,\pi\, a_x/H\,)}\right), \tag{67}$$

and the same methods employed above show that the coefficient of the linear term of the Taylor expansion of this function at $x_1 = a_x$ does vanish (see the Maple code in section 6.3). By symmetry, the results for the expansions at $x_1 = a_x$ and $x_1 = -a_x$ are the same.

5. Conclusions. For two-dimensional problems, a relationship, (2), between the expansions of the primary variable (potential or displacement) on the two sides of a crack tip has been derived. In particular, it has been shown that in the expansion of the crack opening displacement as a function of distance from the tip, there is no linear term present. For fracture mechanics, it should be profitable to exploit this information in either finite or boundary element analyses, improving the accuracy of the near tip fields and, consequently, the stress intensity factors.

While (2) follows from the eigenfunction expansion method, an argument based upon this approach is limited to a traction-free flat crack in an infinite plate. However, the proof based upon a boundary integral representation shows that this result holds for an *arbitrary crack geometry* (i.e., multiple, nonplanar) and equations other than elasticity. In the case of linear elastic fracture mechanics, this is associated with

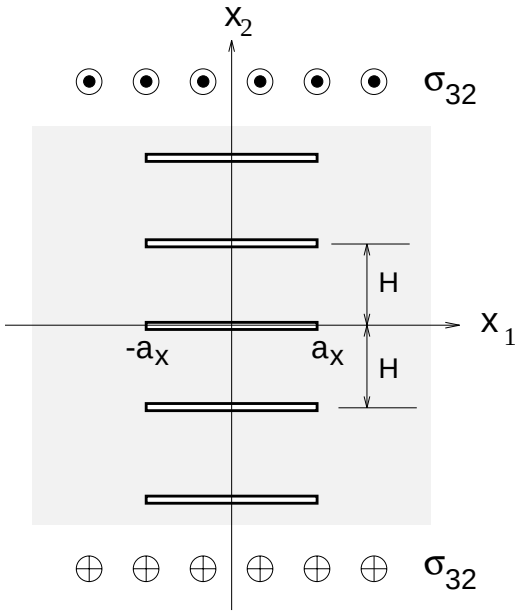

FIG. 8. *Example* 14.1*a from Tada, Paris, and Irwin* [54].

the concept of crack tip autonomy (see Barenblatt [4] and Broberg [11]). This argument is based upon examining the potentially singular terms that arise in evaluating the integral expression for the surface stress near the crack tip. Thus, as in [25], this work illustrates that, rather than ignoring these terms, the potentially singular contributions carry important information and should be examined. Note that the higher-order terms $r^{n/2}$, $n \geq 3$, in the expansion for $\mathbf{u}$ or ϕ yield completely regular integrals, and thus the indication is that no other results along these lines can be expected.

The one assumption employed in the boundary integral argument is that the near tip displacement behavior on the crack surface includes only a square root and a linear term, (34). Note, however, that even if more complicated boundary conditions or geometry (multiple, interacting cracks) should produce a term of the form r^{λ}, $0 < \lambda < 1$ ($\lambda \neq 1/2$), it is unlikely that integration of this term will contribute a logarithmic singularity (i.e., (58)) in the expression for the near tip traction. The argument leading to (2) would therefore remain unaltered.

It is likely that the arguments presented here can be carried over to three-dimensional crack problems. The eigenfunction expansion method has been extended to three dimensions by Benthem [6, 7] and Hartranft and Sih [29], and these results should be applicable. For the more general boundary integral approach, the three-dimensional computations will necessarily be more involved, but based upon the previous analysis of a corner geometry [25], the extension of the limit procedure argument should be more or less straightforward. Work in this direction is currently being pursued. This study will hopefully lead to accurate evaluation of stress intensity factors, and also contribute to a better understanding of the three-dimensional character of the stress distribution in the neighborhood of the crack front.

6. Appendix. The following codes were run with Maple V, release 3. Only a few basic Maple operations, integration and substitution, are employed, and thus it is

likely that, with relatively minor changes, these scripts would work with other symbolic computation systems. The naming of variables follows the notation in this paper fairly closely, and it is therefore hoped that the codes are mostly self-explanatory. However, a few comment lines, which begin with the pound sign (#), are also included. As in section 3, the Laplace equation integrations will be considered first.

6.1. Laplace equation. All of the calculations share a common piece of coding which set up the geometry and the components of the Green's function. Note that the $-(2\pi)^{-1}$ factor in (36) is omitted.

```
# geometry
r1  := ax*x + eps;
r2 := - del;
rh2 := r1**2 + r2**2;
N1 := 0;
N2 := 1;
n1 := 0;
n2 := 1;
jn1 := 0;
jn2 := ax;
# kernel
jnr := jn1*r1 + jn2*r2;
jnN := jn1*N1 + jn2*N2;
rN  := r1*N1 + r2*N2;
num1 := -jnN;
num2 := expand(2*jnr*rN);
kernel := num1/rh2 + num2/rh2^2;
```

6.1.1. ϕ Integrals. The additional coding to calculate the constant and linear terms is

```
t0int := int(kernel,x=-1..0);
s0 := subs(del=0,t0int);
s0 := subs(ax-eps=ax,s0);
s0 := subs(ax*eps=0,s0);
s0 := subs(eps^2=0,s0);
```

and

```
t1 := expand(kernel*x);
t1int := int(t1,x=-1..0);
s1 := subs(del=0,t1int);
s1 := subs(ax*eps=0,s1);
s1 := subs(ax^2+eps^2=ax^2,s1);
s1 := subs(ln(ax^2)*eps^2=0,s1);
s1 := subs(-2*ln(ax^2)*ax*eps=0,s1);
s1 := subs(2*eps^2=0,s1);
```

As might be expected, somewhat more work is involved for the square root term. To assist Maple in computing this integral, the variable q is introduced to simplify the expressions in the kernel denominators.

```
#
# q = x + eps/ax
#
rh2 := expand(subs(x=q-eps/ax,rh2));
#
kernel := num1/rh2 + num2/rh2^2;
```

```
##
## Square root term sqrt(-x)  -1 < x < 0
##
t0   := sqrt(eps/ax-q)*kernel:
t0int := int(t0,q):
t1 := subs(q=eps/ax,t0int):
t2 := - subs(q=-1+eps/ax,t0int):
t1 := expand(t1):
t2 := expand(t2):
tsq := t1 + t2;
tsq := subs(sqrt(ax^2)=ax,tsq):
tsq := subs(1/sqrt(ax^2)=1/ax,tsq):
# beta = sqrt(eps^2+del^2)
tsq := subs(sqrt(ax^2*(eps^2+del^2))=ax*beta,tsq):
tsq := subs(1/sqrt(ax^2*(eps^2+del^2))=1/(ax*beta),tsq):
tsq := subs(sqrt(ax^2*eps^2+del^2*ax^2)=ax*beta,tsq):
tsq := subs(sqrt(eps^2+del^2)=beta,tsq):
tsq := subs(1/sqrt(eps^2+del^2)=1/beta,tsq):
# Taylor expansion for beta
tsq := subs(2*ax*beta=2*ax*eps+ax*del^2/eps,tsq):
tsq := subs((ax*del^2/eps)^(-3/2)=
      eps^(3/2)/(adel*del^2*ax^(3/2)),tsq):
tsq := subs(1/sqrt(ax*del^2/eps)=
      sqrt(eps)/(adel*sqrt(ax)),tsq):
tsq := subs(4*eps*ax+ax*del^2/eps=4*eps*ax,tsq):
tsq := subs(sqrt(eps*ax)=sqrt(ax)*sqrt(eps),tsq):
tsq := subs(1/sqrt(eps*ax)=1/(sqrt(ax)*sqrt(eps)),tsq):
tsq := subs(beta=eps,tsq):
tsq := subs(del^2=0,tsq):
tsq := subs(4^(1/2)=2,tsq):
tsq := subs(1/(ax+2*ax^(1/2)*eps^(1/2)+eps)=1/ax,tsq):
tsq := subs(1/(ax-2*ax^(1/2)*eps^(1/2)+eps)=1/ax,tsq);
```

6.1.2. Flux integral. The coding for the relatively simple flux integral is

```
JNR := ax*(N1*r1 + N2*r2);
i1 := - JNR/rh2;
a0  := int(i1,x=-1..0);
a0 := subs(1/sqrt(ax^2*del^2)=1/ax*1/adel,a0);
```

6.2. Elasticity. The Maple codes for elasticity basically follow the same procedures as for the Laplace equation. However, the code for the square root term is somewhat more complicated, as computing the limit requires keeping additional terms in the Taylor expansions, (56). The linear and square root calculations for the displacement integral, and the constant term for the traction integral, all share the common piece of coding listed below.

```
rc := array(1..2);
n := array(1..2);
a := array(1..2);
b := array(1..2);
c := array(1..2);
sigma := array(1..2,1..2);
```

```
drdx := array(1..2);
p := array(1..2,1..2,1..2);
s := array(1..2,1..2,1..2);
d := array(1..2,1..2);
#
ay := 0;
d[1,1] := 1;
d[1,2] := 0;
d[2,1] := 0;
d[2,2] := 1;
#
rc[1]  := x*ax + eps;
rc[2]  := x*ay - del;
##
r   := (rc[1]^2 + rc[2]^2)**(1/2);
drdx[1] := rc[1]/r;
drdx[2] := rc[2]/r;
## includes jacobian
n[1] := 0;
n[2] := ax;
drdn  := ax*rc[2]/r;
```

6.2.1. Linear: $u_k = c_k r$.

```
for l from 1 to 2 do
 for k from 1 to 2 do
  for m from 1 to 2 do
p[l,k,m]  := (2*drdn*((1-2*nu)*d[l,k]*drdx[m] +
nu*(d[k,m]*drdx[l] + d[l,m]*drdx[k])
- 4*drdx[l]*drdx[k]*drdx[m]) +
2*nu*(n[l]*drdx[k]*drdx[m]+n[k]*drdx[l]*drdx[m])
+(1-2*nu)*(2*n[m]*drdx[l]*drdx[k]+n[k]*d[l,m]+n[l]*d[k,m])
-(1-4*nu)*n[m]*d[l,k])/(r*r);
##
i1  := x*p[l,k,m];
i1 := expand(i1);
a1  := int(i1,x=-1..0):
a1 := subs(arctan(ax*eps/sqrt(ax^2*del^2))=pi/2,a1);
a1 := subs(arctan(ax*(ax-eps)/sqrt(ax^2*del^2))=pi/2,a1);
a1 := subs(sqrt(ax^2*del^2)=ax*del,a1);
a1 := subs(1/sqrt(ax^2*del^2)=1/(ax*del),a1);
a1 := expand(a1);
a1 := subs(del=0,a1);
a1 := subs(ln(eps)=loge,a1);
a1 := subs(ln(eps^2)=2*loge,a1);
a1 := subs(eps=0,a1);
## singular terms
a1 := collect(a1,loge);
a1 := coeff(a1,loge,1);
a1 := a1*ln(epsilon);
p[l,k,m] := a1;
```

```
  od;
 od;
od;
## stress
## c[1] is the linear coefficient from u_1
sigma[1,2] := p[1,2,1]*c[1] + p[1,2,2]*c[2]:
sigma[2,2] := p[2,2,1]*c[1] + p[2,2,2]*c[2]:
sigma[1,2] := subs(sqrt(eps)=0,sigma[1,2]);
sigma[2,2] := subs(sqrt(eps)=0,sigma[2,2]);
sigma[1,2] := subs(1/(ax+4^(1/2)*sqrt(eps*ax)+eps)=
     1/ax,sigma[1,2]);
sigma[2,2] := subs(1/(ax+4^(1/2)*sqrt(eps*ax)+eps)=
     1/ax,sigma[2,2]);
sigma[1,2] := subs(1/(ax-4^(1/2)*sqrt(eps*ax)+eps)=
     1/ax,sigma[1,2]);
sigma[2,2] := subs(1/(ax-4^(1/2)*sqrt(eps*ax)+eps)=
     1/ax,sigma[2,2]);
```

6.2.2. Square root: $u_k = b_k r^{1/2}$.

```
for l from 1 to 2 do
 for k from 1 to 2 do
  for m from 1 to 2 do
p[l,k,m]  := (2*drdn*((1-2*nu)*d[l,k]*drdx[m] +
nu*(d[k,m]*drdx[l]+d[l,m]*drdx[k])-4*drdx[l]*drdx[k]*drdx[m])
+ 2*nu*(n[l]*drdx[k]*drdx[m]+n[k]*drdx[l]*drdx[m])
+(1-2*nu)*(2*n[m]*drdx[l]*drdx[k]+n[k]*d[l,m]+n[l]*d[k,m])
-(1-4*nu)*n[m]*d[l,k])/(r*r);
p[l,k,m]  :=  expand(subs(x=q-eps/ax,p[l,k,m]));
##
i1  := sqrt(eps/ax-q)*p[l,k,m];
i1 := expand(i1);
t1  := int(i1,q):
b1 := ( subs(q=eps/ax,t1) - subs(q=-1+eps/ax,t1) );
b1 := subs(sqrt(ax^2)=ax,b1):
b1 := subs(1/sqrt(ax^2)=1/ax,b1):
# beta = sqrt(eps^2+del^2)
b1 := subs(eps^2+del^2=beta^2,b1);
b1 := expand(b1):
b1 := subs((ax^2*beta^2)^(1/2)=ax*beta,b1):
b1 := subs((beta^2)^(1/2)=beta,b1):
b1 := subs((beta^2)^(-1/2)=1/beta,b1):
b1 := subs((beta^2)^(3/2)=beta^3,b1):
b1 := subs((beta^2)^(-3/2)=1/beta^3,b1):
b1 := subs((beta^2)^(5/2)=beta^5,b1):
b1 := subs((beta^2)^(-5/2)=1/beta^5,b1):
b1 := expand(b1):
b1 := subs((ax*del^2/eps)^(-1/2)=eps^(1/2)/(adel*ax^(1/2)),b1):
b1 := subs((ax*del^2/eps)^(-3/2)=
     eps^(3/2)/(adel*del^2*ax^(3/2)),b1):
b1 := subs((ax*del^2/eps)^(-5/2)=
     eps^(5/2)/(adel*del^4*ax^(5/2)),b1):
```

```
b1 := subs(2*ax*beta+2*eps*ax=4*eps*ax*(1+del^2/eps^2/4),b1);
# Taylor expansion for beta = eps*sqrt(1+del^2/eps^2)
b1 := subs(2*ax*beta-2*eps*ax=ax*del^2/eps,b1);
b1 := expand(b1):
b1 := subs((ax*del^2/eps)^(-1/2)=eps^(1/2)/(adel*ax^(1/2)),b1):
b1 := subs((ax*del^2/eps)^(-3/2)=
     eps^(3/2)/(adel*del^2*ax^(3/2)),b1):
b1 := subs((ax*del^2/eps)^(-5/2)=
     eps^(5/2)/(adel*del^4*ax^(5/2)),b1);
b1 := subs((ax^2)^(3/2)=ax^3,b1);
b1 := subs((eps*ax)^(-3/2)=eps^(-3/2)*ax^(-3/2),b1);
b1 := subs((eps*ax)^(-1/2)=eps^(-1/2)*ax^(-1/2),b1);
b1 := subs(beta=eps*(1+del^2/eps^2/2),b1);
p[l,k,m] := b1;
  od;
 od;
od;
##
## stress
## b[1] is the sqrt coefficient from u_1
##
sigma[1,2] := p[1,2,1]*b[1] + p[1,2,2]*b[2]:
sigma[2,2] := p[2,2,1]*b[1] + p[2,2,2]*b[2]:
##
for j from 1 to 2 do
sigma[j,2] := subs( 4^(1/2)=2,sigma[j,2]):
sigma[j,2] := subs(ax*del^2/eps=tc1,sigma[j,2]):
sigma[j,2] := subs(eps*ax*(1+del^2/(4*eps^2))=tc2,sigma[j,2]):
sigma[j,2] := subs(arctan( (2*ax+2*sqrt(tc2))/sqrt(tc1))=
pi/2,sigma[j,2]):
sigma[j,2] := subs(arctan( (2*ax-2*sqrt(tc2))/sqrt(tc1))=
pi/2,sigma[j,2]):
sigma[j,2] := normal(sigma[j,2]):
sigma[j,2] :=
subs( ln((2*ax*eps+2*sqrt(ax*(4*eps^2+del^2)/eps)*eps+
      2*eps^2+del^2)/(2*eps))=ln(ax)+1+2*sqrt(ax/eps),sigma[j,2]):
sigma[j,2] :=
subs( ln((2*ax*eps-2*sqrt(ax*(4*eps^2+del^2)/eps)*eps+
2*eps^2+del^2)/(2*eps))=ln(ax)+1-2*sqrt(ax/eps),sigma[j,2]):
#
sigma[j,2] := subs( (-ax*del^2*(-4*eps^2+del^2)/eps^3)^(-5/2)=
ax^(-5/2)*del^(-5)*(4*eps^2-del^2)^(-5/2)*eps^(15/2),sigma[j,2]):
sigma[j,2] := subs( (ax*del^2*(4*eps^2-del^2)/eps^3)^(-5/2)=
ax^(-5/2)*del^(-5)*(4*eps^2-del^2)^(-5/2)*eps^(15/2),sigma[j,2]):
sigma[j,2] := subs( (ax*(4*eps^2+del^2)/eps)^(-5/2)=
ax^(-5/2)*(4*eps^2+del^2)^(-5/2)*eps^(5/2),sigma[j,2]):
sigma[j,2] := subs( (-4*eps^2+del^2)^(-2)=
                      (4*eps^2-del^2)^(-2),sigma[j,2]):
sigma[j,2] := subs( (4*eps^2+del^2)^(-9/2)=
(16*eps^4-del^4)^(-9/2)/(4*eps^2-del^2)^(-9/2),sigma[j,2]):
```

```
#
sigma[j,2] := subs(
(2*eps*ax-2*sqrt(ax*(4*eps^2+del^2)/eps)*eps+2*eps^2+del^2)^(-2)
=2^(-2)*eps^(-2)*(sqrt(ax)-sqrt(eps))^(-2),sigma[j,2]):
sigma[j,2] := subs(
(2*eps*ax+2*sqrt(ax*(4*eps^2+del^2)/eps)*eps+2*eps^2+del^2)^(-2)
=2^(-2)*eps^(-2)*(sqrt(ax)+sqrt(eps))^(-2),sigma[j,2]):
sigma[j,2] := subs((sqrt(ax)+sqrt(eps))^(-2)=
(ax-eps)^(-2)/(sqrt(ax)-sqrt(eps))^(-2),sigma[j,2]):
sigma[j,2] := subs( (2*eps^2+del^2)^(-5)=
(1-5*del^2/eps^2/2)*2^(-5)*eps^(-10),sigma[j,2]):
sigma[j,2] := subs( (16*eps^4-del^4)^(-9/2)=
(1+9*del^4/eps^4/32)*16^(-9/2)*eps^(-18),sigma[j,2]):
sigma[j,2] := subs( 16^(1/2)=4,sigma[j,2]):
sigma[j,2] := subs( (ax-eps)^(-2)=ax^(-2),sigma[j,2]):
sigma[j,2] := expand(sigma[j,2]):
#
sigma[j,2] := subs( (4*eps*ax+ax*del^2/eps)^(9/2) =
4^(9/2)*eps^(9/2)*ax^(9/2)*(1+9*del^2/eps^2/8),sigma[j,2]):
sigma[j,2] := subs( (4*eps*ax+ax*del^2/eps)^(7/2) =
4^(7/2)*eps^(7/2)*ax^(7/2)*(1+7*del^2/eps^2/8),sigma[j,2]):
sigma[j,2] := subs( (4*eps*ax+ax*del^2/eps)^(5/2) =
4^(5/2)*eps^(5/2)*ax^(5/2)*(1+5*del^2/eps^2/8),sigma[j,2]):
sigma[j,2] := subs( (4*eps*ax+ax*del^2/eps)^(3/2) =
4^(3/2)*eps^(3/2)*ax^(3/2)*(1+3*del^2/eps^2/8),sigma[j,2]):
sigma[j,2] := subs( (4*eps*ax+ax*del^2/eps)^(1/2) =
4^(1/2)*eps^(1/2)*ax^(1/2)*(1+del^2/eps^2/8),sigma[j,2]):
#
sigma[j,2] := subs( (4*ax*del^2/eps-ax*del^4/eps^3)^(9/2)=
(1+9*del^2/eps^2/8)*ax^(9/2)*del^9*(4/eps)^(9/2),sigma[j,2]):
sigma[j,2] := subs( (4*ax*del^2/eps-ax*del^4/eps^3)^(7/2)=
(1+7*del^2/eps^2/8)*ax^(7/2)*del^7*(4/eps)^(7/2),sigma[j,2]):
sigma[j,2] := subs( (4*ax*del^2/eps-ax*del^4/eps^3)^(5/2)=
(1+5*del^2/eps^2/8)*ax^(5/2)*del^5*(4/eps)^(5/2),sigma[j,2]):
sigma[j,2] := subs( (4*ax*del^2/eps-ax*del^4/eps^3)^(3/2)=
(1+3*del^2/eps^2/8)*ax^(3/2)*del^3*(4/eps)^(3/2),sigma[j,2]):
sigma[j,2] := expand(sigma[j,2]):
sigma[j,2] := subs(del=0,sigma[j,2]):
sigma[j,2] := subs( (1/eps)^(5/2)=eps^(-5/2),sigma[j,2]):
sigma[j,2] := normal(sigma[j,2]):
sigma[j,2] := subs(eps=0,sigma[j,2]):
od;
#
sigma[1,2];
sigma[2,2];
```

6.2.3. Traction integral.

```
for l from 1 to 2 do
 for k from 1 to 2 do
  for m from 1 to 2 do
```

```
s[l,k,m]  := ( (1-2*nu)*(drdx[k]*d[l,m] + drdx[l]*d[k,m] -
drdx[m]*d[l,k]) + 2*drdx[l]*drdx[k]*drdx[m] )/r;
##
i1  := s[l,k,m];
i1 := expand(i1);
t1  := int(i1,x=-1..0):
t1  := subs((ax^2*del^2)^(-1/2)=1/(ax*adel),t1);
t1  := subs((ax^2*del^2)^(-1/2)=1/(ax*adel),t1);
t1 := subs(arctan(eps/adel)=pi/2,t1);
t1 := subs(arctan((ax-eps)/adel)=pi/2,t1);
t1 := expand(t1);
s[l,k,m] := t1;
  od;
 od;
od;
##
## stress
## a[1] is the constant coefficient from tau_1
##
sigma[1,2] := s[1,2,1]*a[1] + s[1,2,2]*a[2];
sigma[2,2] := s[2,2,1]*a[1] + s[2,2,2]*a[2];
sigma[1,2] := subs(del=0,sigma[1,2]);
sigma[2,2] := subs(del=0,sigma[2,2]);
sigma[1,2] := subs(log(eps^2)=loge,sigma[1,2]);
sigma[2,2] := subs(log(eps^2)=loge,sigma[2,2]);
sigma[1,2] := subs(eps=0,sigma[1,2]);
sigma[2,2] := subs(eps=0,sigma[2,2]);
```

6.3. Exact solutions. Listed below is the coding employed to evaluate the linear term coefficient for the four examples in section 4.

```
##
## Example 5.10 from Tada et al. (1985)
## aa = 1/(a-b)  bb = b/(a*(a-b))
##
#f := arccosh((1+bb*s^2)/(1-aa*s^2));
##
## Example 7.1a from Tada et al. (1985)
##
#f := arccosh(cos(pi*(ax-s^2)/w)/cos(pi*ax/w));
##
## Example 7.4a from Tada et al. (1985)
## pw = pi/w
##
#g1 := 1 - (cos(a*pw)/cos(pw*(a-s^2)))^2;
#g2 := 1 - (cos(a*pw)/cosh(pw*y0))^2;
#g  := sqrt(g1/g2);
#f1 := arctanh(g);
#f2 := diff(f1,y0);
#f := f1 - alpha*y0*f2;
```

```
##
## Example 14.1a from Tada et al. (1985)
## ph = pi/H
##
#g1 := cosh((a-s^2)*ph);
#g2 := cosh(a*ph);
#g := g1/g2;
#f := arccos(g);
##
## This is the common piece of coding for all four problems
##
d1 := diff(f,s);
d2 := diff(d1,s);
d2 := normal(d2);
num := numer(d2);
den := denom(d2);
####     Extra statements for Example 14.1a
#num := subs(cosh(a*ph)=(exp(a*ph)+exp(-a*ph))/2,num);
#num := subs(sinh(a*ph)=(exp(a*ph)-exp(-a*ph))/2,num);
#num := expand(num);
#den := subs(cosh(a*ph)=(exp(a*ph)+exp(-a*ph))/2,den);
#den := subs(sinh(a*ph)=(exp(a*ph)-exp(-a*ph))/2,den);
#den := expand(den);
####
num := series(num,s=0,8):
num := convert(num,polynom):
num := expand(num);
den := series(den,s=0,9):
den := convert(den,polynom):
den := expand(den);
d2 := normal(num/den);
d2 := subs(s=0,d2);
```

Acknowledgments. The authors would like to thank Professors S. Mukherjee and A. Ingraffea of Cornell University for helpful discussions. The second author would like to thank Dr. R. F. Sincovec for hospitality at Oak Ridge National Laboratory while this work was performed.

REFERENCES

[1] M. H. Aliabadi and D. P. Rooke, *Numerical Fracture Mechanics*, Computational Mechanics Publications and Kluwer Academic Publishers, Southampton and Dordrecht, 1991.

[2] I. Babuška, T. V. Petersdorff, and B. Andersson, *Numerical treatment of vertex singularities and intensity factors for mixed boundary value problems for the Laplace equation in R^3*, SIAM J. Numer. Anal., 31 (1994), pp. 1265–1288.

[3] L. Banks-Sills, *Application of the finite element method to linear elastic fracture mechanics*, Appl. Mech. Rev., 44 (1991), pp. 447–461.

[4] G. I. Barenblatt, *The formation of equilibrium cracks during brittle fracture. General ideas and hypotheses. Axially-symmetric cracks*, Appl. Math. Mech. (PMM, USSR), 23 (1959), pp. 622–636.

[5] R. S. Barsoum, *On the use of isoparametric finite elements in linear fracture mechanics*, Internat. J. Numer. Methods Engrg., 10 (1976), pp. 25–37.

[6] J. P. Benthem, *State of stress at the vertex of a quarter-infinite crack in a half-space*, Internat. J. Solids Structures, 13 (1977), pp. 479–492.
[7] J. P. Benthem, *The quarter-infinite crack in a half space: Alternative and additional solutions*, Internat. J. Solids Structures, 16 (1980), pp. 119–130.
[8] G. E. Blandford, A. R. Ingraffea, and J. A. Liggett, *Two-dimensional stress intensity factor computations using the boundary element method*, Internat. J. Numer. Methods Engng, 17 (1981), pp. 387–404.
[9] V. G. Blinova and A. M. Linkov, *A method of finding asymptotic forms at the common apex of elastic wedges*, Appl. Math. Mech. (PMM, USSR), 59 (1995), pp. 187–195.
[10] C. A. Brebbia, J. C. F. Telles, and L. C. Wrobel, *Boundary Element Techniques*, Springer-Verlag, Berlin, New York, 1984.
[11] K. B. Broberg, *The foundations of fracture mechanics*, Engrg. Fract. Mech., 16 (1982), pp. 497–515.
[12] J. S. Bullock, G. E. Giles, and L. J. Gray, *Simulation of an electrochemical plating process*, in Topics in Boundary Element Research, Vol. 7, C. A. Brebbia, ed., Springer-Verlag, Berlin, New York, 1990, pp. 121–141.
[13] B. K. Char, K. O. Geddes, G. H. Gonnet, and S. M. Watt, *Maple User's Guide*, WATCOM Publications Ltd., University of Waterloo, Waterloo, Canada, 1985.
[14] E. G. Coker and L. N. G. Filon, *A Treatise on Photo-Elasticity*, 2nd ed., Cambridge University Press, Cambridge, 1957.
[15] S. L. Crouch and A. M. Starfield, *Boundary Element Methods in Solid Mechanics*, George Allen and Unwin, London, 1983.
[16] T. A. Cruse, *Boundary Element Analysis in Computational Fracture Mechanics*, Kluwer Academic Publishers, Boston, 1988.
[17] T. A. Cruse, *Three-dimensional elastic surface cracks*, in Fracture Mechanics: Nineteenth Symposium, ASTM STP 969, T. A. Cruse, ed., American Society for Testing and Materials, Philadelphia, 1988, pp. 19–42.
[18] T. A. Cruse and G. Novati, *Traction BIE formulations and applications to non-planar and multiple cracks*, in Fracture Mechanics: Twenty Second Symposium, Vol. II, ASTM STP 1131, S. N. Atluri, J. C. Newman, I. S. Raju, and J. S. Epstein, eds., American Society for Testing and Materials, Philadelphia, 1992, pp. 314–332.
[19] A. H. England, *On stress singularities in linear elasticity*, Internat. J. Engrg. Sci., 9 (1971), pp. 571–585.
[20] N. A. Fleck, J. W. Hutchinson, and Z. Suo, *Crack path selection in a brittle adhesive layer*, Internat. J. Solids Structures, 27 (1991), pp. 1683–1703.
[21] Y. C. Fung, *Foundations of Solid Mechanics*, Prentice-Hall, Englewood Cliffs, NJ, 1965.
[22] L. J. Gray, *Boundary element method for regions with thin internal cavities*, Engrg. Anal. Boundary Elem., 6 (1989), pp. 180–184.
[23] L. J. Gray, *Symbolic computation of hypersingular boundary integrals*, in Advances in Boundary Element Techniques, J. H. Kane, G. Maier, N. Tosaka, and S. N. Atluri, eds., Springer-Verlag, Berlin, Heidelberg, 1993, pp. 157–172.
[24] L. J. Gray, C. Balakrishna, and J. H. Kane, *Symmetric Galerkin boundary integral fracture analysis*, Engrg. Anal. Boundary Elements, 15 (1995), pp. 103–109.
[25] L. J. Gray and E. D. Lutz, *On the treatment of corners in the boundary element method*, J. Comput. Appl. Math., 32 (1990), pp. 369–386.
[26] L. J. Gray and L. L. Manne, *Hypersingular boundary integrals at a corner*, Engrg. Anal. Boundary Elem., 11 (1993), pp. 327–334.
[27] L. J. Gray, L. F. Martha, and A. R. Ingraffea, *Hypersingular integrals in boundary element fracture analysis*, Internat. J. Numer. Methods Engrg., 29 (1990), pp. 1135–1158.
[28] R. D. Gregory, *Green's functions, bi-linear forms, and completeness of the eigenfunctions for the elastostatic strip and wedge*, J. Elasticity, 9 (1979), pp. 283–309.
[29] R. J. Hartranft and G. C. Sih, *The use of eigenfunction expansions in the general solution of three-dimensional crack problems*, J. Math. Mech., 19 (1969), pp. 123–138.
[30] R. D. Henshell and K. G. Shaw, *Crack tip finite elements are unnecessary*, Internat. J. Numer. Methods Engrg., 9 (1975), pp. 495–507.
[31] H. K. Hong and J. T. Chen, *Derivation of integral equations in elasticity*, J. ASCE, Eng. Mech. Div., 114 (1988), pp. 1028–1044.
[32] Á. Horváth, *Higher-order singular isoparametric elements for crack problems*, Comm. Numer. Methods Engrg., 10 (1994), pp. 73–80.
[33] A. I. Kalandiia, *Remarks on the singularity of elastic solutions near corners*, Appl. Math. Mech. (PMM, USSR), 33 (1969), pp. 127–131.

[34] S. N. Karp and F. C. Karal, Jr., *The elastic-field behavior in the neighborhood of a crack of arbitrary angle*, Comm. Pure Appl. Math., XV (1962), pp. 413–421.
[35] V. A. Kondrat'ev, *Boundary problems for elliptic equations in domains with conical or angular points*, Trans. Moscow Math. Soc., (Moskovskoe matematicheskoe obshchestvo), 16 (1967), pp. 227–313.
[36] I. L. Lim, I. W. Johnston, and S. K. Choi, *Application of singular quadratic distorted isoparametric elements in linear fracture mechanics*, Internat. J. Numer. Methods Engrg., 36 (1993), pp. 2473–2499.
[37] A. M. Linkov and S. G. Mogilevskaya, *Hypersingular integrals in plane problems of elasticity*, Appl. Math. Mech. (PMM, USSR), 54 (1990), pp. 93–99.
[38] E. D. Lutz and L. J. Gray, *Exact evaluation of singular boundary integrals without CPV*, Comm. Numer. Methods Engrg., 9 (1993), pp. 909–915.
[39] D. E. Medina and J. A. Liggett, *Three dimensional boundary element computation of potential flow in fractured rock*, Internat. J. Numer. Methods Engrg., 26 (1988), pp. 2319–2330.
[40] N. I. Muskhelishvili, *Some Basic Problems of the Mathematical Theory of Elasticity*, 4th ed., P. Noordhoff, Groningen, The Netherlands, 1963.
[41] G. H. Paulino, M. T. A. Saif, and S. Mukherjee, *A finite elastic body with a curved crack loaded in anti-plane shear*, Internat. J. Solids Structures, 30 (1993), pp. 1015–1037.
[42] J. R. Rice, *Mathematical analysis in the mechanics of fracture*, in Fracture: An Advanced Treatise, Vol. II, H. Liebowitz, ed., Pergamon Press, Oxford, 1968, pp. 191–311.
[43] F. J. Rizzo, *An integral equation approach to boundary value problems of classical elastostatics*, Quart. Appl. Math., 25 (1967), pp. 83–95.
[44] R. Rösel, *On the wedge/notch eigenvalues*, Internat. J. Fracture, 33 (1987), pp. 61–71.
[45] D. Rosen and D. E. Cormack, *Singular and near singular integrals in the BEM: A global approach*, SIAM J. Appl. Math., 53 (1993), pp. 340–357.
[46] D. Rosen and D. E. Cormack, *The continuation approach: A general framework for the analysis and evaluation of singular and near-singular integrals*, SIAM J. Appl. Math., 55 (1995), pp. 723–762.
[47] S. Selcuk, D. S. Hurd, S. L. Crouch, and W. Gerberich, *Prediction of interfacial crack path: A direct boundary integral approach and experimental study*, Internat. J. Fracture, 67 (1994), pp. 1–20.
[48] A. M. Shapiro and J. Andersson, *Steady state fluid response in fractured rock: A boundary element solution for a coupled, discrete fracture continuum model*, Water Resources Research, 19 (1983), pp. 959–969.
[49] J. Sladek and V. Sladek, *Dynamic stress intensity factors studied by boundary integro-differential equations*, Internat. J. Numer. Methods Engrg., 23 (1986), pp. 919–928.
[50] I. N. Sneddon and H. A. Elliott, *The opening of a Griffith crack under internal pressure*, Quart. Appl. Math., 4 (1946), pp. 262–267.
[51] J. L. Sousa, *Three-dimensional Simulation of Near-Wellbore Phenomena Related to Hydraulic Fracturing from a Perforated Wellbore*, Ph.D. thesis, Cornell University, Ithaca, NY, 1992.
[52] O. D. L. Strack and H. M. Haitjema, *Modeling double aquifer flow using a comprehensive potential and distributed singularities* 1: *Solution for homogeneous permeability*, Water Resources Research, 17 (1981), pp. 1535–1549.
[53] B. A. Szabó and I. Babuška, *Computation of the amplitude of stress singular terms for cracks and reentrant corners*, in Fracture Mechanics: Nineteenth Symposium, ASTM STP 969, T. A. Cruse, ed., American Society for Testing Materials, Philadelphia, 1988, pp. 101–124.
[54] H. Tada, P. C. Paris, and G. R. Irwin, *The Stress Analysis of Cracks Handbook*, 2nd ed., Paris Productions Inc. and Del Research Corp., Missouri, 1985.
[55] D. M. Tracey, *Finite elements for determination of crack tip elastic stress intensity factors*, Engrg. Frac. Mech., 3 (1971), pp. 255–265.
[56] D. Vasilopoulos, *On the determination of higher order terms of singular elastic stress fields near corners*, Numer. Math., 53 (1988), pp. 51–95.
[57] M. L. Williams, *Stress singularities resulting from various boundary conditions in angular corners of plates in extension*, ASME J. Appl. Mech., 19 (1952), pp. 526–528.
[58] M. L. Williams, *On the stress distribution at the base of a stationary crack*, ASME J. Appl. Mech., 24 (1957), pp. 109–114.